

Evaluation of the RMMAC/XI Method with Time-Varying Parameters and Disturbance Statistics

P. Rosa*, M. Athans*[§], S. Fekri[‡], C. Silvestre*

*Institute for Systems and Robotics/Instituto Superior Técnico, Lisbon, Portugal

[§]M. Athans is also Professor of EECS (emeritus), M.I.T., U.S.A.

[‡]Control and Instrumentation Research Group, University of Leicester, Leicester, UK

Emails: {prosa, athans, -, cjs}@isr.ist.utl.pt, sf111@le.ac.uk

Abstract—We demonstrate, using Monte-Carlo simulations, the robust performance of the adaptive control methodology denoted by RMMAC/XI introduced and discussed in Refs. [1-3]. The RMMAC/XI architecture can handle simultaneous time-variations in the plant uncertain parameters as well as the disturbance intensity statistics. We compare the RMMAC/XI performance vs that of the best possible robust nonadaptive design using the same physical example described in Refs. [1-4]. Whenever possible, we also compare the RMMAC/XI performance with that of the (unrealizable) “Perfect Model Identification (PM.ID)” introduced in [4].

Index Terms—Robust adaptive control, multiple-model adaptive control, time-varying uncertain plant parameters, time-varying disturbance statistics

I. INTRODUCTION

This paper evaluates the “Robust Multiple-Model Adaptive Control (RMMAC/XI)” architecture, depicted in Fig. 1, for a mass-spring-dashpot (MSD) test example subject to simultaneous time-variation of the uncertain spring stiffness and unknown disturbance intensity – see Fig. 2. This architecture was introduced in Refs. [1-4]. The interested reader is referred to Refs. [1-4] for more detail.

The performance of the MSD system subject to time-varying uncertain parameters but constant disturbance intensity was evaluated in our previous work ([4]), for which the RMMAC could perform a perfect performance. The main difference between this paper and [4] relies on having a disturbance with time-varying intensity, which requires the use of an extension of the RMMAC methodology, referred to as RMMAC/XI. In this architecture, we may consider different disturbance intensities. For instance, we can assume that plants with spring stiffness within a certain interval can either be described by model #P or model #P+N, depending on the disturbance intensity, say Ξ_1 or Ξ_2 , respectively. Note that in Refs. [1-4] model #P was designed considering the disturbance intensity Ξ_1 , and considering Ξ_2 for model #P+N.

This work was partially supported by Fundação para a Ciência e a Tecnologia (FCT), ISR/IST pluriannual funding, through the POS_Conhecimento Program that includes FEDER funds. The work of P. Rosa was supported by a PhD Student Grant from the FCT.

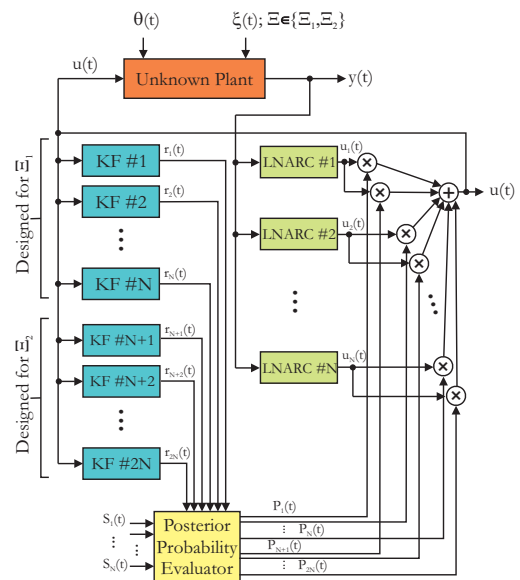


Fig. 1. RMMAC/XI architecture with N dynamic models

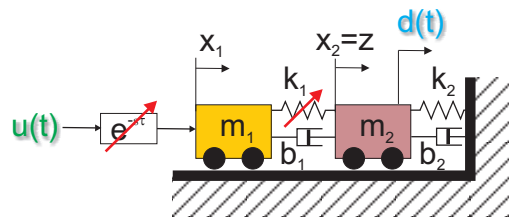


Fig. 2. MSD system with uncertain spring constant, k_1 , and disturbances denoted by $d(t)$. $u(t)$ is the control input and $z(t)$ is the system output. τ is an uncertain time-delay bounded by $0 < \tau < 0.05$ s, as in [1-2].

In this paper, the RMMAC/XI identification subsystem consists of $2N$ Kalman filters (KFs) followed by a “Posterior Probability Evaluator (PPE)”. It was not clear, from Refs. [1-4], what the posterior probabilities were when the disturbance intensity was unknown during design stage or when it was changing in time (fast or slowly). In order to evaluate the performance of the RMMAC/XI architecture, we compare it, whenever possible, to that associated with “Perfect Model Identification (PM.ID.)” with local nonadaptive robust controllers (LNARCs). Also, a comparison to the performance of the *best* global nonadaptive robust controller (GNARC) is presented in this paper. As

in [4], two different cases are analyzed in this paper: the first, for a low frequency control bandwidth case (previously designed in [1]); the second, which is a much harder control problem, for a higher control bandwidth (previously designed in [2]).

Each dynamic model and covariance matrix, $cov[\xi(t); \xi(\tau)] = E\{\xi(t)\xi'(\tau)\} = \Xi\delta(t - \tau)$, of the continuous-time zero-mean plant white noise $\xi(t)$, have associated one KF, where Ξ is the plant-noise intensity matrix.

The disturbance force $d(t)$ shown in Fig. 2 is a stationary colored stochastic process that results from the output of a first order low-pass filter. This transfer function, $W_d(s)$, has a pole at $s = \alpha$ and is driven driven with continuous-time white noise $\xi(t)$, with zero mean and intensity Ξ .

II. LOW-FREQUENCY DESIGN (LFD) SIMULATIONS

In this section a set of 4 simulations are presented for the LFD design case. We consider $\alpha = 0.1$ rad/s, and RMMAC/XI controller design choices and performance requirements are as presented in [1-3]. The simulation results were obtained from 5 Monte-Carlo runs.

Table I shows the respective spring constant interval and disturbance intensity for each design case. The regions for the spring constant are chosen according to [3], so the performance of the RMMAC/XI is not below 70% of the fixed nonadaptive robust controller (FNARC), as explained in detail in [1-3]. Eight models are obtained, four associated to disturbance intensity, $\Xi = 1$, and four associated to disturbance intensity $\Xi = 100$.

TABLE I
LFD RMMAC/XI MODEL DEFINITIONS

Model # for $\Xi = 1$	Model # for $\Xi = 100$	Spring Constant Interval
#1	#5	$\Omega_1 = [1.02 \ 1.75]$
#2	#6	$\Omega_2 = [0.64 \ 1.02]$
#3	#7	$\Omega_3 = [0.4 \ 0.64]$
#4	#8	$\Omega_4 = [0.25 \ 0.4]$

Case 1 (LFD): k_1 Waveform A, $\Xi = \{1, 100\}$ (Waveform AX)

Next, we consider a case where the disturbance intensities take one of two predefined values, as in [3] and as it can be seen in Fig. 4. We also consider the spring stiffness with step changes, depicted in Fig. 3. The probability transients are shown in Fig. 5, from which it can be concluded that the transitions are not as fast as in the case where the disturbance intensities are constant (see, for instance, [3] or [4]). Nonetheless, this identification problem does not avoid the improved performance of the RMMAC/XI when compared with the GNARC. This can be concluded from Fig. 6 and Table II.

The last two columns of Table II show the following percentage comparisons:

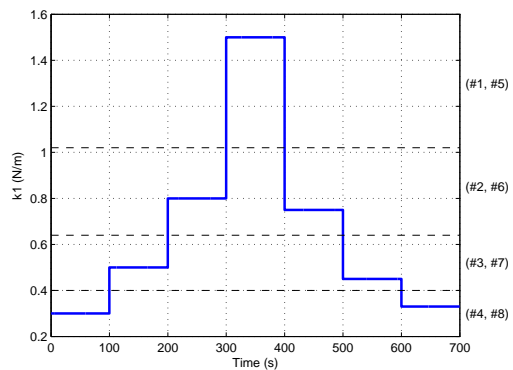


Fig. 3. Waveform A: Time-varying spring constant, k_1

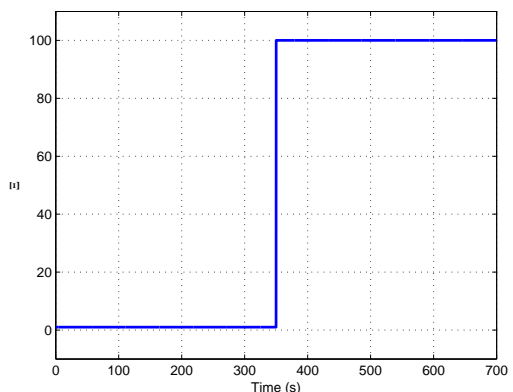


Fig. 4. Waveform AX: Disturbances power, Ξ

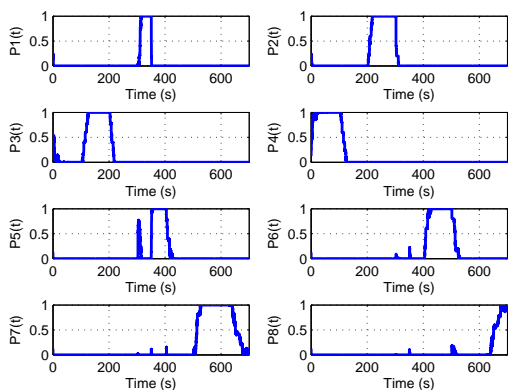


Fig. 5. Probability transients, $P_k(t)$, for k_1 waveform A and Ξ waveform AX

$$\%E = \frac{RMMAC/XI\,value - PM.ID.\,value}{PM.ID.\,value} \quad (1)$$

$$\%F = \frac{GNARC\,value - RMMAC/XI\,value}{RMMAC/XI\,value}$$

Although the RMMAC/XI RMS performance is lower than the one achieved by the PM.ID. scheme, it is still remarkably above the one obtained with a nonadaptive controller. In the second part of the simulation (high disturbance intensity), there is an improvement in terms of RMS performance. This is mainly due to the fact that higher intensity disturbances help the identification procedure resulting in faster probability transients and in control laws closer to those selected in the PM.ID case.

Case 2 (LFD): $k_1 = 0.28$, Ξ Waveform BX

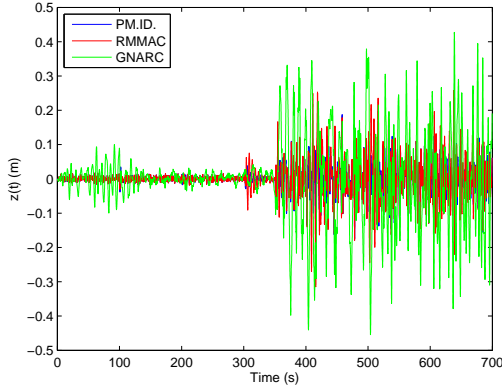


Fig. 6. Mass position, $z(t)$, for k_1 waveform A and Ξ waveform AX

TABLE II

CASE 1 (LFD) RMS AND MEAN VALUES OF $z(t)$

Time Interval	[0 350]	[350 700]
Mean RMMAC/XI	6.22e-5	-8.56e-5
Mean PM.ID.	5.84e-5	-5.32e-5
Mean GNARC	1.34e-3	-2.34e-3
RMS RMMAC/XI	1.26e-4	5.39e-3
RMS PM.ID.	5.20e-5	2.87e-3
RMS GNARC	6.34e-4	2.68e-2
%E Mean	6.4 %	60.8 %
%F Mean	2052.8 %	2633.1 %
%E RMS	143.2 %	87.7 %
%F RMS	401.6 %	397.9 %

Next, the spring constant is fixed to $k_1 = 0.28$ and the disturbance intensity is defined as depicted in Fig. 7. This sinusoidal time-varying Ξ will help to show which one of the two models is selected by the identification process when the disturbance intensity differs from the predefined values.

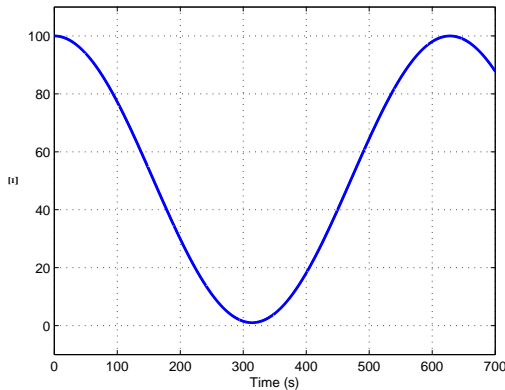


Fig. 7. Waveform BX: Sinusoidal time-varying disturbances power, Ξ

Figure 8 shows that only if Ξ is roughly below 10, the identification procedure considers the correct model to be in the first KF set ($\Xi = 1$). Table III presents the performance improvement of using adaptive control. From the table it can be readily seen that indeed we have a RMS performance gain of about 24. As explained in [3], the LNARCs used in the RMMAC/XI controller do not depend on the disturbance intensity. Hence, the LNARC

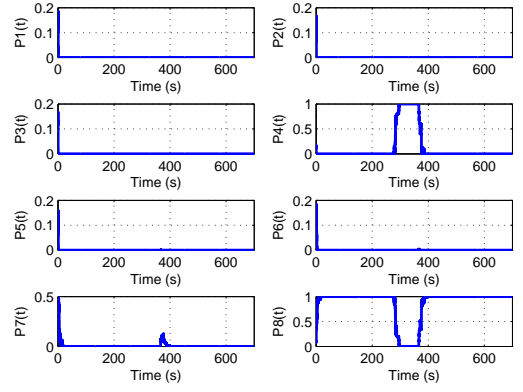


Fig. 8. Probability transients, $P_k(t)$, for $k_1 = 0.28$ and Ξ waveform BX

used for model #1 is the same used for model #5, the one used for model #2 is the same used for model #6, and so on. Therefore, it is not important, for control purposes, if the identification procedure picks model #4 or #8 as far as one of them is selected. This justifies the overall quality of the results obtained. However, it is very worthwhile to mention that to guarantee a certain level of performance the transition between these two models should occur in such way that the remaining models present always negligible posterior probabilities.

TABLE III

CASE 2 (LFD) RMS AND MEAN VALUES OF $z(t)$

	RMMAC/XI	GNARC	%F
Mean	8.41e-5	9.05e-4	975.8 %
RMS	1.93e-3	4.92e-2	2443.6 %

Case 3 (LFD): k_1 Waveform C and Ξ Waveform BX

Now we discuss a much harder problem. The spring stiffness is assumed to be sinusoidal as shown in Fig. 9 and $\Xi(t)$ is the same as in Case 2. The behavior of the RMMAC/XI can be judged from the results illustrated in Fig. 10 and Table IV. The probabilities convergence is slower than in the previous tests, as expected, since we are changing not only a system parameter but also the disturbance intensity, turning out a much difficult task for the estimation algorithm. Due to the misbehavior of the identification technique, we do not have the same performance improvement as before, when comparing the RMMAC/XI results with those of the GNARC. Nonetheless, the gain of about 6 is obtained for the overall RMS performance.

TABLE IV

CASE 3 (LFD) RMS AND MEAN VALUES OF $z(t)$

	RMMAC/XI	GNARC	%F
Mean	6.74e-5	7.15e-4	961.1 %
RMS	2.60e-3	1.99e-2	667.4 %

Case 4 (LFD): k_1 Waveform C and Ξ Waveform CX

Finally, an even harder case is analyzed. In the previous case, we had the disturbance intensity within the predefined values, $\Xi \in [1, 100]$. Here we assume that

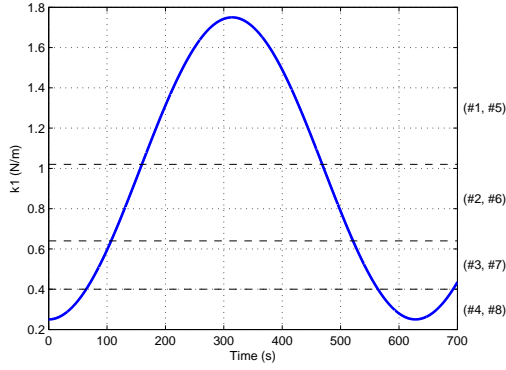


Fig. 9. Waveform C: Sinusoidal time-varying spring constant, k_1

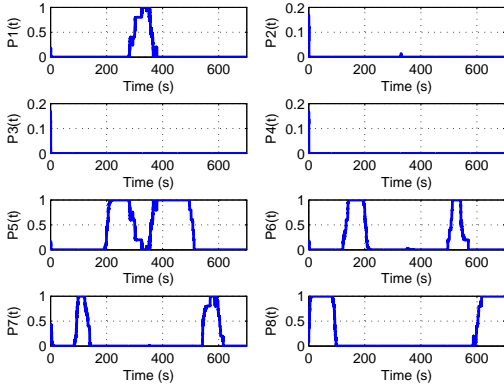


Fig. 10. Probability transients, $P_k(t)$, for k_1 waveform C and Ξ waveform BX

Ξ exceeds these boundaries, as shown in Fig. 11. This should be more difficult for the probabilistic estimation algorithm to identify the correct model. However, this may not necessarily result in a loss of performance. In fact, when relating the results regarding the comparison between the RMMAC/XI and the GNARC and previous tests, we have a slight improvement in terms of RMS gain, as presented in Table V. Figure 12 shows the misbehavior of identification process which does not degrade the performance of the closed loop system.

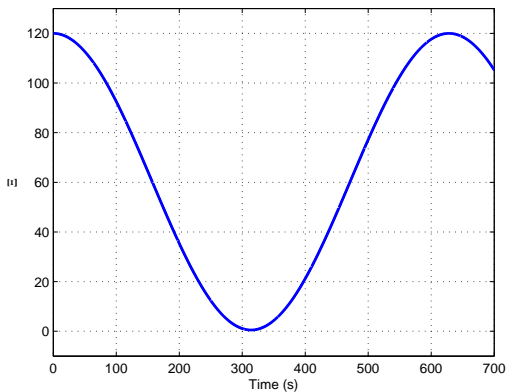


Fig. 11. Waveform CX: Sinusoidal disturbances power, Ξ

III. HIGH-FREQUENCY DESIGN SIMULATIONS

In this section, a more challenging control problem is discussed. Although we use the same MSD system for the

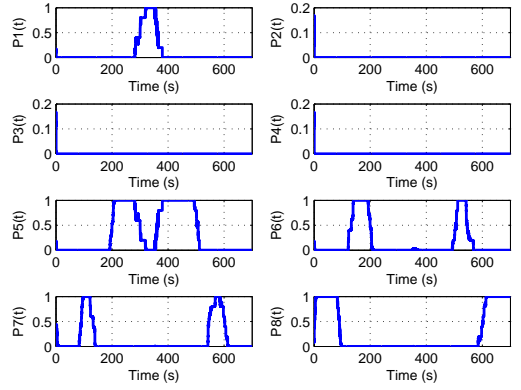


Fig. 12. Probability transients, $P_k(t)$, for k_1 waveform C and Ξ waveform CX

TABLE V
CASE 4 (LFD) RMS AND MEAN VALUES OF $z(t)$

	RMMAC/XI	GNARC	%F
Mean	6.73e-5	6.75e-4	903.7 %
RMS	2.97e-3	2.38e-2	701.4 %

performance evaluation of the RMMAC/XI methodology, we now consider a higher frequency range with $\alpha = 3$ rad/s. Thus, the disturbance force $d(t)$ has significant power over a larger frequency range, leading to the excitation of all the lightly-damped modes of the MSD system. In order to compensate for the disturbances with the new extended frequency range, a controller with wider bandwidth is required.

The details of the HFD RMMAC/XI methodology for this case are given in [2]. This problem reveals several difficulties when it comes to the identification of the correct model, as will be seen in the sequel. In order to achieve the same performance specifications as in [2], we use 14 models ($2N=14$), corresponding to 7 models for each Ξ , as described in Table VI.

TABLE VI
HFD RMMAC/XI MODEL DEFINITIONS

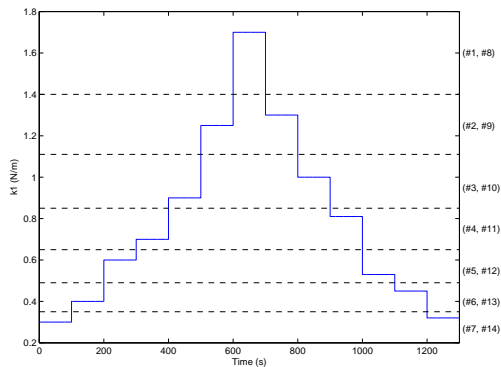
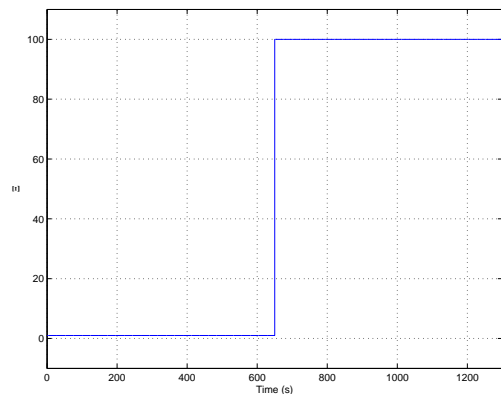
Model # for $\Xi = 1$	Model # for $\Xi = 100$	Spring Constant Interval
#1	#8	$\Omega_1 = [1.4 \ 1.75]$
#2	#9	$\Omega_2 = [1.11 \ 1.4]$
#3	#10	$\Omega_3 = [0.85 \ 1.11]$
#4	#11	$\Omega_4 = [0.65 \ 0.85]$
#5	#12	$\Omega_5 = [0.49 \ 0.65]$
#6	#13	$\Omega_6 = [0.35 \ 0.49]$
#7	#14	$\Omega_7 = [0.25 \ 0.35]$

Simulation results for the different situations are presented next, using 5 Monte-Carlo runs for each case.

Case 5 (HFD): k_1 Waveform D, $\Xi = \{1, 100\}$ (Waveform DX)

Similarly to Case 1, k_1 has step changes, but with waveform D, illustrated in Fig. 13. The waveform of Ξ is also similar to the one of Case 1, as shown in Fig. 14, but now the step occurs at a different time.

Figure 16 presents the output of the system for the three

Fig. 13. Waveform D: Time-varying spring constant, k_1 Fig. 14. Waveform DX: Disturbances power, Ξ

controllers considered. From the Fig. 16 and Table VII, one can see that there are significant RMS performance improvements when comparing the RMMAC/XI to the *best* nonadaptive controller. However, there is still a substantial loss of RMS performance when comparing with the PM.ID. This can again be explained by the misbehavior of the identification process – see Fig. 15.

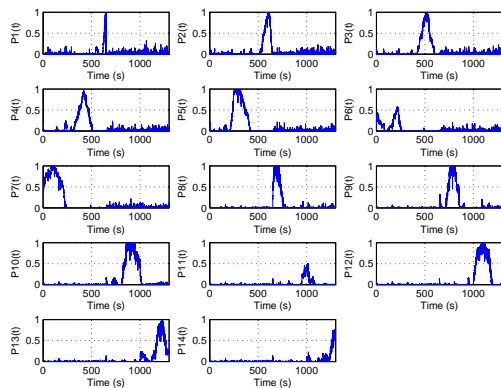
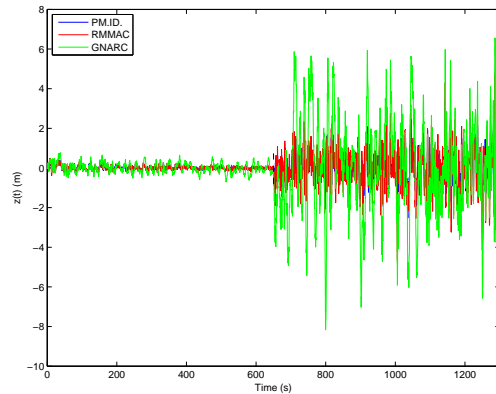
Fig. 15. Probability transients, $P_k(t)$, for k_1 waveform D and Ξ waveform DX

Table VII also shows that, as in Case 1, a higher loss of performance from the PM.ID to the RMMAC/XI occurs when the disturbance intensity is smaller.

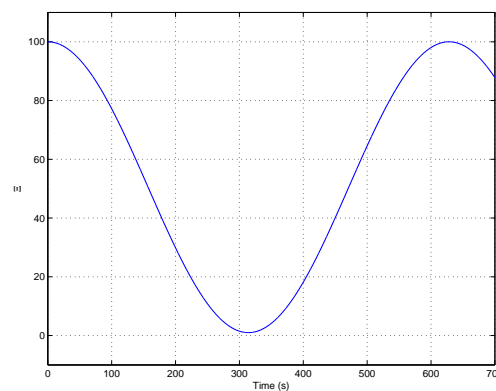
Case 6 (HFD): $k_1 = 0.57$, Ξ Waveform EX

We now consider the HFD RMMAC/XI simulation similar to the Case 2. We use the spring stiffness $k_1 = 0.57$ (the correct models are Model #5 when $\Xi=1$ or

Fig. 16. Output, $z(t)$, for k_1 waveform D and Ξ waveform DXTABLE VII
CASE 5 (HFD) RMS AND MEAN VALUES OF $z(t)$

Time Interval	[0 650]	[650 1300]
Mean RMMAC/XI	6.67e-3	-3.69e-2
Mean PM.ID.	6.46e-3	-1.87e-2
Mean GNARC	7.19e-3	-6.25e-2
RMS RMMAC/XI	1.41e-2	1.09
RMS PM.ID.	1.02e-2	7.48e-1
RMS GNARC	6.07e-2	5.89
%E Mean	3.3 %	97.5 %
%F Mean	7.9 %	69.7 %
%E RMS	38.6 %	46.1 %
%F RMS	329.2 %	439.1 %

Model #12 when $\Xi = 100$) and waveform EX, as shown in Fig. 17, for the disturbance intensity. As illustrated in Fig. 18, the probability transients are not as well behaved as in the LFD case. This means that the RMS performance gain from the GNARC to the RMMAC/XI should be smaller than for the LFD case, due to the misbehavior of model identification procedure. This can be concluded based upon Table VIII.

Fig. 17. Waveform EX: Disturbances power, Ξ

Nonetheless, we attain a RMS performance gain of about 3.4 resulting from the use of adaptive control, despite the problems found during the estimation process.

Case 7 (HFD): k_1 Waveform F and Ξ Waveform EX

In this case, we use the same waveform for $\Xi(t)$ as before, and waveform F for the spring stiffness, $k_1(t)$.

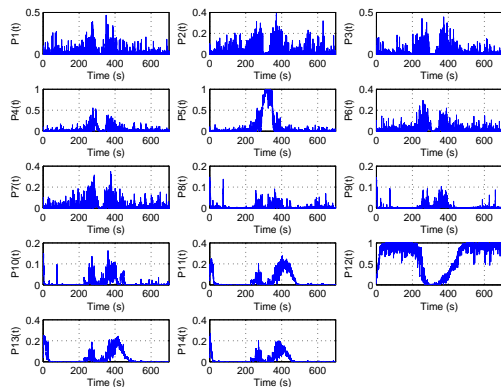


Fig. 18. Probability transients, $P_k(t)$, for $k_1 = 0.57$ and Ξ waveform EX

TABLE VIII

CASE 6 (HFD) RMS AND MEAN VALUES OF $z(t)$

	RMMAC/XI	GNARC	%F
Mean	-2.26e-2	-1.03e-1	355.8 %
RMS	7.19e-1	3.20	345.3 %

Waveform F is a sinusoidal wave between 0.25 and 1.75 with frequency one third of that of the disturbance intensity. The probability transients are depicted in Fig. 19. As expected, the identification process is somewhat “confused”, since we have time-variations on both the system parameter and the disturbance intensity. Table IX shows a significant gain on the RMS performance due to the adaptive control law exploited.

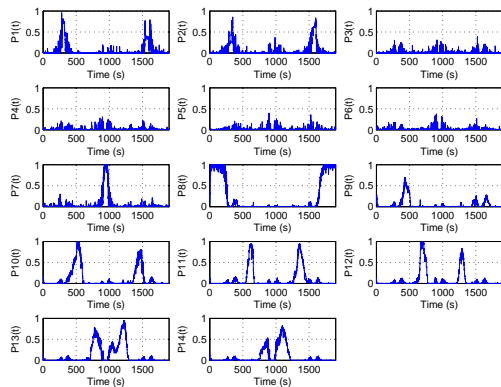


Fig. 19. Probability transients, $P_k(t)$, for k_1 waveform F and Ξ waveform EX

TABLE IX

CASE 7 (HFD) RMS AND MEAN VALUES OF $z(t)$

	RMMAC/XI	GNARC	%F
Mean	-6.43e-3	-2.25e-2	249.2 %
RMS	5.00e-1	2.96	492.8 %

Case 8 (HFD): k_1 Waveform F and Ξ Waveform FX

Similar to previous case, we now use Waveform F for the spring stiffness. However, for this case, the disturbance intensity varies between 0.5 and 120. The results are shown in Fig. 20 and Table X.

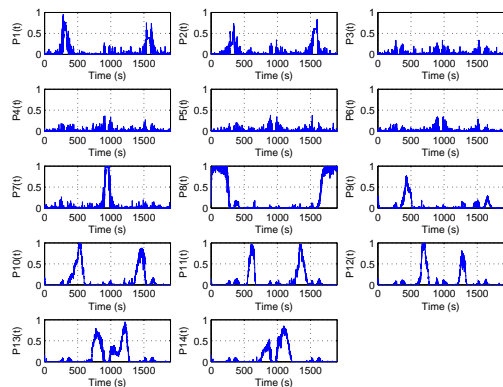


Fig. 20. Probability transients, $P_k(t)$, k_1 waveform F and Ξ waveform FX

TABLE X

CASE 8 (HFD) RMS AND MEAN VALUES OF $z(t)$

	RMMAC/XI	GNARC	%F
Mean	-7.91e-3	-2.46e-2	211.6 %
RMS	6.28e-1	3.53	463.1 %

Despite the violation of several theoretical assumptions required for the design of the RMMAC/XI, we still obtain RMS performance improvements of about 4.6. This is remarkable since the intensity of the disturbance is time-variant and assumes values different from the ones used in the KFs design stage.

IV. CONCLUSIONS AND FUTURE WORK

This work presented some results turning out that the RMMAC/XI architecture can still have better performance than the GNARC even when the uncertain parameter and the disturbance intensity are simultaneously time-varying. It should be noted that this happens even when the actual disturbance intensity was not considered during design. Hence, the performance of this controller does not depend strictly on the correct model identification, since what matters for control purposes is that the interval of the parameter value is properly identified.

The results presented also show that the violation of several design assumptions does not affect the stability of the closed loop system. Furthermore, the performance of the RMMAC/XI was always clearly above the one of the GNARC demonstrating that significant improvements arise from the use of this adaptive controller.

REFERENCES

- [1] S. Fekri, M. Athans, A. Pascoal, “Issues, progress and new results in robust adaptive control,” *Int. J. of Adaptive Control and Signal Processing*, in press
- [2] S. Fekri, M. Athans, A. Pascoal, “Robust multiple model adaptive control (RMMAC): A case study,” *Int. J. of Adaptive Control and Signal Processing*, 2006, in press
- [3] S. Fekri, “Robust adaptive MIMO control using multiple-model hypothesis testing and mixed- μ synthesis,” Ph.D. dissertation, Instituto Superior Tecnico, Lisbon, Portugal, December 2005
- [4] P. Rosa et al, “Further Evaluation of the RMMAC Method with Time-varying Parameters”, *Proc. Mediterranean Conference on Automation and Control, MED07*, Athens, Greece, June 2007 (submitted)